Journal of Fundamental and Applied Sciences

ISSN 1112-9867

Available online at http://www.jfas.info

EFFECTS OF GEOMETRIC RATIOS AND FIBRE ORIENTATION ON THE NATURAL FREQUENCIES OF LAMINATED COMPOSITE PLATES

B. Attaf* and M. Bachene

Expert in composite materials & structures - France

Received: 05 September 2010 / Accepted: 06 December 2010 / Published online: 31 December 2010

ABSTRACT

The present investigation aims to examine the influence of geometric ratios and fibre orientation on the natural frequencies of fibre-reinforced laminated composite plates using finite element method based on Yang's theory and his collaborators. The transverse shear and rotatory inertia effects were taken into consideration in the developed Fortran computer program. It has been shown that the use of first-order displacement field provides the same accuracy as higher-order displacement field when the number of elements representing the plate structure is increased (refined mesh). However, poor precision may appear for plates with high thickness-to-side ratio *h/a* (thickness/side length). This discrepancy limits the application of the developed theory to thick plates (*h/a*<0.5). The various curves show the evolution of the dimensionless frequency (ω*) *versus* fibre orientation angle (θ) and illustrate the apparition of a "triple-point" phenomenon engendered by the increase of the plate aspect ratio *a/b* (length/width) for a specific value of *h/a*. This point defines the maximum natural frequency and the associated fibre orientation. Also, results show that for high and/or low aspect ratios, the triple-point phenomenon does not occur. This latter is rapidly reached for thick plates than thin plates when the plate aspect ratio *a/b* is progressively increased.

Keywords: composite plates, dimensionless frequency, fibre orientation, finite element method, geometric ratios, triple-point.

Author Correspondence, e-mail: b.attaf@wanadoo.fr

ICID: 1020796

1. INTRODUCTION

In addition to the choice of material and manufacturing process in the design of fibre-reinforced composite plates, a search for an adequate stacking sequence and proper fibre orientation is an important step provided to achieve an efficient structural performance coupled with an optimal design [1]. For symmetrically laminates [2], the analysis is simplified and the achievement of an optimised stacking sequence is easily reached. However, for arbitrary laminates the analysis becomes complicated and analytical formulations are unable to yield appropriate results on the vibrational behaviour of such laminates. The complexity of the formulation is mainly due to the presence of coupling parameters and their effects [3-4]. In such situation, the finite element method [5-6] is among the numerical methods that are enabling approximate solutions and providing an optimum design of new materials and structures usually in the form of plates, used as structural key components in different fields of engineering including those operating on water, in space and on earth. These plates must be designed strong enough to perform safely in operating conditions, withstand severe conditions of vibration and stability to which they will be exposed throughout their service life.

As the stacking sequence is an important factor in the design of laminated composite plates, it is therefore necessary to undertake studies on the vibration of these plates in order to predict their natural frequencies and avoid possible resonance phenomena. Within this context, Sirinivas [7], Jones [8] and Noor [9] have initially studied the vibration problem of rectangular thick cross-ply laminated plates with simply supported boundary conditions, where the determination of the fundamental frequencies was based on the use of the three-dimensional elasticity theory. On the other hand, Fortier & Rossettos [10] have analysed the free vibration of rectangular antisymmetric cross-ply laminated plates. Whereas, Bert & Chen [11] have examined the transverse shear effect on the natural frequencies of antisymmetric laminated plates; they have shown that the transverse shear effect cannot be neglected when carrying out analysis on thick plates. Also, Kant & Mallikarjuna [12] have applied the finite element method to investigate the vibration of antisymmetric laminated plates and sandwich panels; their formulation was based on higher-order displacement shape function with neglected transverse shear correction factors. Jing & Liao [13] have undertaken some investigations in hybrid element method using stress fields. Furthermore, in studies conducted by Shiau &

Chang [14], the rotatory inertia effect was neglected and high number of triangular elements with 36 degrees of freedom was used to examine the effect of transverse shear deformation on the natural frequencies. Conclusively, Tesselar et al. [15], Bachene [5] and Mohd Sultan Ibrahim [6] have presented a higher-order theory to analyse the vibration of laminated thick plates.

The objective of the present work is to examine the influence of geometric ratios and fibre orientation on the natural frequencies of laminated rectangular plates and aims to accomplish the work previously conducted by Attaf [16]. For this purpose, a FORmula TRANslator (FORTRAN) computer program was developed enabling to solve difficulties inherent to the problem of vibration analysis. Also, the present method was examined by comparing obtained results with those available in literature [11, 12, 15, 17], this has allowed to validate the theory developed via the computer program. Excluding some no exhaustive indications in Refs. [12], [18] and [14], the literature review shows that little investigations have been made on this subject matter.

2. MATHEMATICAL FORMULATIONS AND FIELD EQUATIONS

A laminated rectangular composite plate with lateral dimensions *a, b* and thickness *h* was considered. The plate Cartesian coordinates are *x*, *y* and *z* , where *x* and *y* lie in the middle surface and *z* is measured from the middle surface. The thickness of the plate is constituted of *n*-plies differently orientated and composed of the same material.

The displacement field used is based on Yang *et al*. theory [19], this is given by the following equations:

$$\begin{aligned} u(x,y,z,t) &= u_0(x,y,t) + z\theta_x(x,y,t) \\ v(x,y,z,t) &= v_0(x,y,t) + z\theta_y(x,y,t) \\ w(x,y,z,t) &= w_0(x,y,t) \end{aligned} \tag{1}$$

where: u, v, w are the displacements along x, y, z directions; u_0, v_0, w_0 are the point displacements located on the middle surface of the plate along x, y, z directions and θ_x, θ_y are the normal rotations to the middle surface about x and y axis, respectively.

Taking into consideration the transverse shear deformations in addition to bending-extension coupling effects, the constitutive equation in the (x,y,z) laminate system can be written as:

$$\begin{Bmatrix} N_x \\ N_y \\ N_{xy} \\ M_x \\ M_y \\ M_{xy} \\ Q_y \\ Q_x \end{Bmatrix} = \begin{bmatrix} A_{11} & A_{12} & A_{16} & B_{11} & B_{12} & B_{16} & 0 & 0 \\ & A_{22} & A_{26} & B_{12} & B_{22} & B_{26} & 0 & 0 \\ & & A_{66} & B_{16} & B_{26} & B_{66} & 0 & 0 \\ & & & D_{11} & D_{12} & D_{16} & 0 & 0 \\ & & & & D_{22} & D_{26} & 0 & 0 \\ & & sym & & & D_{66} & 0 & 0 \\ & & & & & & F_{44} & F_{45} \\ & & & & & & & F_{55} \end{bmatrix} \begin{Bmatrix} \varepsilon_{0x} \\ \varepsilon_{0y} \\ \gamma_{0xy} \\ \kappa_x \\ \kappa_y \\ \kappa_{xy} \\ \gamma_{yz} \\ \gamma_{xz} \end{Bmatrix} \tag{2a}$$

Or in compact matrix form as:

$$\begin{Bmatrix} \{N\} \\ \{M\} \\ \{Q\} \end{Bmatrix}_{x,y} = \begin{bmatrix} [A] & [B] & 0 \\ [B] & [D] & 0 \\ 0 & 0 & [F] \end{bmatrix} \begin{Bmatrix} \{\varepsilon^0\} \\ \{\kappa\} \\ \{\gamma\} \end{Bmatrix}_{x,y} \tag{2b}$$

in which *N*, *M* and *Q* are the force, moment and transverse shear vectors and ε^0, κ and γ are the associated strains and curvatures vectors, respectively. The coefficients A_{ij} (extensional stiffnesses), B_{ij} (coupling stiffnesses), D_{ij} (bending stiffnesses) and F_{ij} (transverse shear stiffnesses) are expressed as [3]:

$$(A_{ij}, B_{ij}, D_{ij}) = \sum_{k=1}^{n} \int_{z_{k-1}}^{z_k} (\overline{Q}_{ij})_k (1, z, z^2) dz, \qquad (i, j = 1, 2, 6) \tag{3}$$

and,

$$F_{ij} = \alpha_{ij} \sum_{k=1}^{n} \int_{z_{k-1}}^{z_k} (\overline{Q}_{ij})_k dz, \qquad (i, j = 4, 5) \tag{4}$$

where α_{ij} are the transverse shear correction factors, taken equal to 5/6 in this analysis.

3. FINITE ELEMENT FORMULATIONS

The analysis is based on a *nine-node isoparametric quadrilateral element*. Each node possesses 5 independent degrees of freedom (three displacements *u*, *v*, *w* and two rotations θ_x, θ_y). Thus, the elementary displacement field can be defined by the following matrix expression [20-21]:

$$\begin{Bmatrix} u_0 \\ v_0 \\ w_0 \\ \theta_x \\ \theta_y \end{Bmatrix} = \sum_{i=1}^{9} \begin{bmatrix} N_i & 0 & 0 & 0 & 0 \\ 0 & N_i & 0 & 0 & 0 \\ 0 & 0 & N_i & 0 & 0 \\ 0 & 0 & 0 & N_i & 0 \\ 0 & 0 & 0 & 0 & N_i \end{bmatrix} \begin{Bmatrix} u_{0i} \\ v_{0i} \\ w_{0i} \\ \theta_{xi} \\ \theta_{yi} \end{Bmatrix} \tag{5a}$$

After some rearrangements, Equation (5a) may be written in compact matrix form as:

$$\{a\} = [N]\{a_e\} \tag{5b}$$

where $[N]=[N_1\ N_2\ \ N_9]$ is the displacement shape function matrix expressed in terms of natural coordinates (ξ, η), and $\{a_e\}=\{\{d_1\}\ \{d_2\}\ \ \{d_9\}\}$ is the nodal displacement vector. The elementary strain-displacement relationship can be obtained from Equation (5) that is as follows:

$$\begin{Bmatrix} \varepsilon_{0x} \\ \varepsilon_{0y} \\ \gamma_{0xy} \\ \kappa_x \\ \kappa_y \\ \kappa_{xy} \\ \gamma_{xz} \\ \gamma_{yz} \end{Bmatrix} = \sum_{i=1}^{9} \begin{bmatrix} \partial N_i/\partial x & 0 & 0 & 0 & 0 \\ 0 & \partial N_i/\partial y & 0 & 0 & 0 \\ \partial N_i/\partial y & \partial N_i/\partial x & 0 & 0 & 0 \\ 0 & 0 & 0 & \partial N_i/\partial x & 0 \\ 0 & 0 & 0 & 0 & \partial N_i/\partial y \\ 0 & 0 & 0 & \partial N_i/\partial y & \partial N_i/\partial x \\ 0 & 0 & \partial N_i/\partial x & N_i & 0 \\ 0 & 0 & \partial N_i/\partial y & 0 & N_i \end{bmatrix} \begin{Bmatrix} u_{0i} \\ v_{0i} \\ w_{0i} \\ \theta_{xi} \\ \theta_{yi} \end{Bmatrix} \tag{6a}$$

Or in compact matrix form as:

$$\{\varepsilon\} = [B]\{a_e\} \tag{6b}$$

where $[B]=[B_1\ B_2\ \ B_9]$ is the interpolation matrix of deformation.

Using the Lagrange equation, it is easy to derive the differential equation of laminated composite plates under free vibration, where the eigenvalue solutions can be obtained by solving the following equations of motion:

$$([K] - \omega^2 [M])\{a_0\} = \{0\} \tag{7}$$

where $[K]$ is the plate global stiffness matrix, $[M]$ is the plate global mass matrix, $\{a_0\}$ is the global displacement vector and ω is the plate natural frequency ($\omega=2\pi f$).

The global stiffness matrix and the global mass matrix are obtained by assembling the elementary stiffness matrices $[K_e]$ and mass matrices $[M_e]$; these are given by the following:

$$[K_e]=\int_{\Omega_e}[B]^T[C][B]\,d\Omega_e \qquad (8)$$

$$[M_e]=\int_{\Omega_e}[N]^T[\overline{m}][N]\,d\Omega_e \qquad (9)$$

where Ω_e is the elementary surface and $[\overline{m}]$ is the inertia matrix; they are expressed as:

$$[\overline{m}]=\begin{bmatrix} I_0 & 0 & 0 & I_1 & 0 \\ 0 & I_0 & 0 & 0 & I_1 \\ 0 & 0 & I_0 & 0 & 0 \\ I_1 & 0 & 0 & I_2 & 0 \\ 0 & I_1 & 0 & 0 & I_2 \end{bmatrix} \qquad \text{with: } I_i=\sum_{k=1}^{n}\int_{z_{k-1}}^{z_k} z^i \rho^k dz \quad \text{and} \quad i=0,1,2$$

To solve Equation (7), a computer program was developed to search the eigenvalues and eigenmodes (*i.e.*, natural frequencies and mode shapes) for free vibration problem. The calculation of stiffness and mass matrices has been performed using selective integration procedure and Lobatto's method [22], respectively. On the other hand, the well-known subspace iteration method [23] was used to solve the eigenproblem.

4. APPLICATION EXAMPLES

4.1. Validation of the computer program

To verify the accuracy of the developed program, a comparative study between the first eleven natural frequency values obtained by other available approaches and the present approach was established. Two laminated square plates (specially antisymmetric and cross-ply symmetric) were considered. The boundary conditions are those associated to a simply supported plate; these are:

- at: $x = 0, a$ $\quad u_0=w_0=\theta_y=0$
- at: $y = 0, b=a$ $\quad v_0=w_0=\theta_x=0$

The material mechanical characteristics are typical to those of carbon/epoxy composites; these are given as follows:

$E_1/E_2 = 40.$ $\quad G_{12}/E_2 = G_{13}/E_2 = 0.6$ $\quad G_{23}/E_2 = 0.5$ $\quad \nu_{12} = 0.25$

The plate was divided into 10×10 elements, which corresponds to 441 nodes representing the entire domain.

For the composite laminated plate with stacking sequence [45°/-45°/45°/-45°], the plate thickness-to-side ratio (*h/a*) is kept constant and equal to 0.1. The first eleven eigenvalues (see Table 1) are compared with results available in Ref.[11] (*i.e.*, Closed form solution) and Ref.[12] (*i.e.*, Higher–Order Shear–deformation Theory HOST). Errors shown in the last column of Table 1 are estimated according to Ref.[11].

For the case of composite laminated plate with stacking sequence [0°/90°/90°/0°], the plate thickness-to-side ratio (*h/a*) is variable from 0.001 to 0.50. The results shown in Table 2 were compared with those available in Ref.[15] and Ref.[17]. Errors are estimated according to Ref.[15], they can be minimised and reduced if refined meshes are used.

Tableau 1. Dimensionless frequency $\omega^* = \omega\, a^2 \sqrt{\rho / E_2\, h^2}$ for antisymmetric angle-ply [45°/-45°/45°/-45°] of simply supported square plate with thickness-to-side ratio *h/a*=0.1

M	*n*	Present Analysis	Bert & Chen Ref.[11]	HOST Ref.[12]	Error / to Ref.[11]
1	1	18.46	18.46	18.32	0.00
1	2	34.87	34.87	34.54	0.00
2	2	50.51	50.52	49.71	-0.02
1	3	54.27	54.27	53.63	0.00
2	3	67.13	67.17	65.02	-0.06
1	4	75.55	75.28	75.65	0.36
3	3	82.72	82.84	83.14	-0.14
2	4	85.15	85.27	86.75	-0.14
1	5	97.45	97.56	99.45	-0.11
3	4	98.73	99.02	100.88	-0.29
2	5	104.67	104.95	103.28	-0.27

Tableau 2. Dimensionless frequency $\omega^* = \omega\, a^2 \sqrt{\rho / E_2\, h^2}$ for symmetric cross-ply laminate [0°/90°/90°/0°] of simply supported square plate

h/a	Present analysis	Tesseler & *al.* Ref.[15]	Approach solution [17]	Error / to Ref.[15]
0.50	5.499	5.260	5.576	-4.54
0.25	9.394	9.224	9.497	-1.84
0.20	10.853	10.748	10.989	-0.98
0.10	15.142	15.149	15.270	0.05
0.08	16.186	16.187	16.276	0.01
0.05	17.659	17.626	17.668	-0.19
0.04	18.071	18.023	18.050	-0.27
0.02	18.674	18.605	18.606	-0.37
0.01	18.836	18.753	18.755	-0.44
0.001	18.891	18.805	---	-0.46

4.2. Effect of fibre orientation on the first natural frequency (Fig.1)

Laminates in the form of rectangular plates with eight unidirectional plies alternatively orientated as follows [θ/-θ/θ/-θ/θ/-θ/θ/-θ] have been considered. The mechanical characteristics and the boundary conditions are the same as those used previously for the plate with thickness-to-side ratio h/a equals to 0.1.

The dimensionless frequency value $\omega^* = \omega a^2 \sqrt{\rho / E_2\, h^2}.10$ is calculated according to the fibre orientation angle θ and the different values of the plate aspect ratio *a/b*. For each value of *a/b*, the variation of ω* *versus* θ is represented in the form of graph. The resulting various graphs are illustrated in Figure 1, from which the following features may be distinguished:

- for a plate aspect ratio *a/b* <1, the dimensionless frequency ω* decreases when the lamination angle θ increases;
- for a plate aspect ratio *a/b* =1, the dimensionless frequency ω* increases slightly in the interval [0°; 45°] to reach its maximum value at θ = 45°, then decreases approximately with the same slope in the interval [45°; 90°];

- for a plate aspect ratio 1<*a/b*≤10, the dimensionless frequency ω* increases in the interval [0°; θ_a] to reach its maximum value at $\theta=\theta_a$, then decreases continually in the interval [θ_a, 70°]. The point corresponding to $\theta=\theta_a$ is called *''triple-point for natural frequencies''*. The curve representing the function *f*(θ)=ω* is continuous at $\theta=\theta_a$, but not differentiable at that point. The lamination angle θ_a depends systematically on the plate aspect ratio *a/b*;
- for a plate aspect ratio *a/b*>12, the dimensionless frequency ω* reaches its maximum value at θ=0°, then decreases rationally when θ increases. The graph of ω* as a function of θ is continuous and differentiable on the entire interval [0°; 90°]. The triple-point phenomenon does not occur.

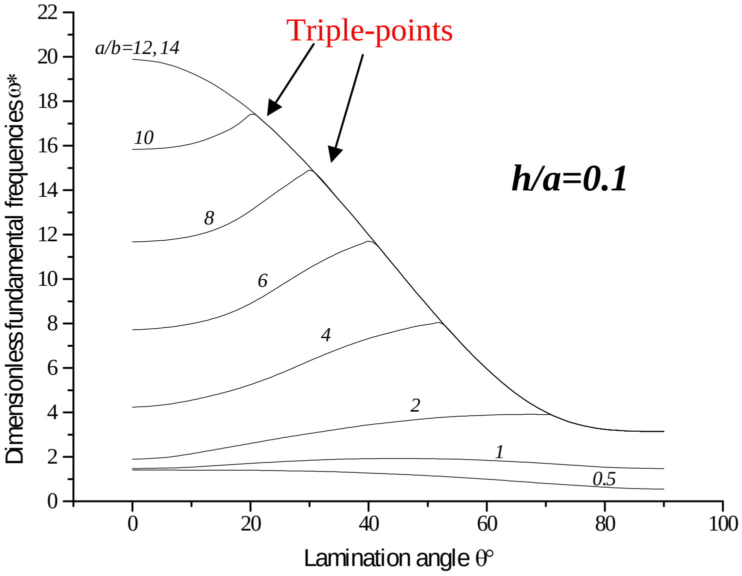

Fig.1. Dimensionless frequency $\omega^* = \omega\, a^2 \sqrt{\rho / E_2 h^2}.10$ *vs.* lamination angle θ; for different plate aspect ratios *a/b* with laminate stacking sequence [θ/-θ/θ/-θ/θ/-θ/θ/-θ] and thickness-to-side ratio *h/a*=0.1

According to Figure 1, it can be concluded that for a plate aspect ratio *a/b*>12, the maximal value of ω* is always reached at θ=0°; further increase of the ratio *a/b* beyond 12 does not affect the dimensionless frequency ω*. The triple-point corresponding to the abscissa θ_a characterises the maximum rigidity of the plate, for which all fibres are orientated at θ_a . In such situation, it may be assumed that the behaviour of a laminated composite plate is the same as a quasi-isotropic plate. The triple-point phenomenon is not discernable when the plate aspect ratio *a/b* is less than or equal to1.

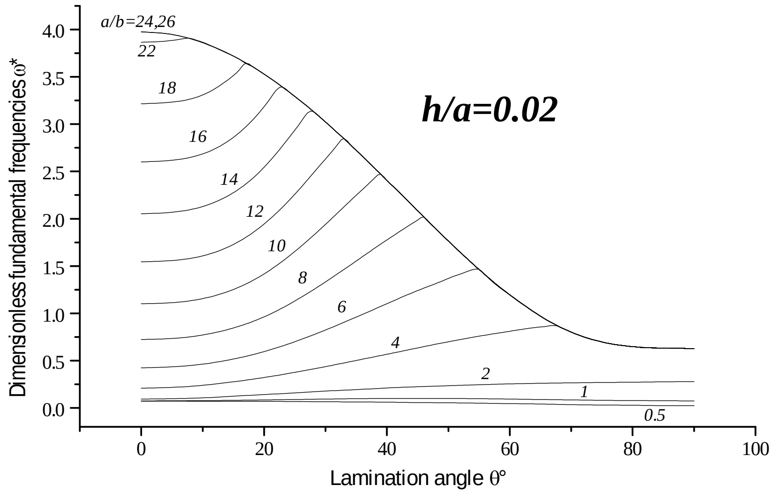

Fig.2. As Fig.1, with thickness-to-side ratio *h/a*=0.02

To generalise the previous observations made for a plate with thickness-to-side ratio *h/a*=0.1, a thin plate with thickness-to-side ratio *h/a*=0.02 was considered. The corresponding results are illustrated in Figure 2. It can be seen that the variation of the dimensionless frequency ω* *vs.* lamination angle, θ, for different values of *a/b* yields similar observations to those discussed previously in Figure 1, except that locations of various triple-points are different and the function $f(\theta)=\omega^*$ is totally continuous and differentiable for a plate with aspect ratio $a/b \geq 24$: interval in which the phenomenon of triple-point does not appear. By comparing the results shown in Figure 1 with those shown in Figure 2, it can be seen that the triple-point position for natural frequencies depends also on the plate thickness-to-side ratio *h/a*.

To further generalise the analysis, Figure 3 shows numerical results for the case of a thick plate with thickness-to-side ratio, *h/a*, equals to 0.2. The dimensionless frequency curve ω* *vs.* θ (Figure 3) behaves differently from the two cases previously examined (*i.e.*, Figs.1 & 2). For a plate aspect ratio *a/b* equals 8 to10, the triple-point is not reached and the maximal dimensionless frequency ω* is equal to 27.5241; this corresponds to a lamination angle θ equals to 29°. For a plate aspect ratio *a/b*≤1, the triple-point phenomenon does not occur within this interval and dissimilarities can easily be discerned in Figure 3.

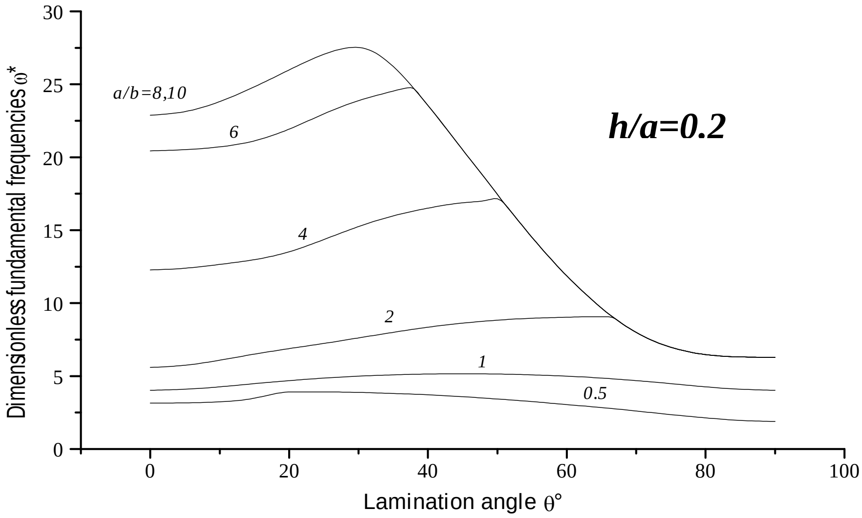

Fig.3. As Fig.1, with thickness-to-side ratio *h/a*=0.2

5. CONCLUSION

The influence of geometric ratios (plate aspect ratio *a/b* and its thickness-to-side ration *h/a*) and fibre orientation on the first natural frequencies of antisymmetric laminated composite plates was examined. It was shown that the use of first-order displacement field yields the same accuracy as higher-order displacement field when the number of elements representing the plate structure is increased (refined mesh) and also when the integration technique used for calculating the stiffness and mass matrices is performed. Poor precision may appear for plates with high thickness-to-side ratio *h/a* (thickness/length side). This discrepancy limits the application of the developed theory to thick plates with thickness-to-side ratio *h/a* less than 0.5.

The present analysis has shown that the increase of the plate aspect ratio *a/b* leads to the apparition of a triple-point phenomenon within a specific interval of fibre orientation for which the natural frequencies can reach their maximum values. The triple-point is rapidly reached for thick plates than thin plates when increasing the plate aspect ratio *a/b* and it does not occur for high and low plate aspect ratios. Finally, it can be concluded that the shape of the curve ω* *versus* θ and the triple-point positions depend significantly on the laminate stacking sequence, the fibre orientation angle and the plate dimensions (thickness, length and width).

6. REFERENCES

[1] Fares, M E. *et al*., Optimal design and control of composite laminated plates with various boundary conditions using various plate theories, Composites Structures, vol. 56, n°1, 1-12 (2002)

[2] Gurses M. *et al*., Free vibration analysis of symmetric laminated skew plates by discrete singular convolution technique based on first-order shear deformation theory, Int. Journal for Numerical Methods in Eng., Vol. 79, n°3, 290-313 (2009)

[3] Jones R M., *Mechanics of composite materials*. Taylor & Francis, Inc., Philadelphia (1999)

[4] Saarela O., Computer programs for mechanical analysis and design of polymer matrix composites. Prog. Polym. Sci. Vol.19, 58-60 (1994)

[5] Bachene M., Analyse modale des plaques composites stratifiées épaisses par la méthode des éléments finis, Mémoire de Magistère en mécanique, Université de Blida, Algérie (2000)

[6] Mohd Sultan Ibrahim S D., Free vibration analysis of laminated composite plates based on higher order shear deformation theory using finite element method, MSc Thesis, International Islamic University Malaysia (2002)

[7] Srinivas S., Joga Rao C V. & Rao A K., An exact analysis for vibration of simply-supported homogeneous and laminated thick rectangular plates, J. Sound Vib. 12, 187-199 (1970)

[8] Jones A T., Exact natural frequencies for cross-ply laminates, J. Comp. Mat., 4, 476-491 (1970)

[9] Noor A K., Free vibrations of multilayered composite plates, AIAA. J. 11, 1938-1939 (1973)

[10] Fortier R C. and Rossettos J N., On the vibration of shear deformable curved anisotropic composite plates, J. Appl. Mech. 40, 299 (1973)

[11] Bert C W. and Chen T L C., Effect of shear deformation on vibration of antisymmetric angle-ply laminated rectangular plates, Int. J. Solids Struct., 14, 465-473 (1978)

[12] Kant T. and Mallikarjuna, A higher-order theory for free vibration of unsymmetrically laminated composite and sandwich plates – finite element evaluations, Comput. Struct. 32(5), 1125-1132 (1989)

[13] Jing H S. and Liao M L., Partial hybrid stress element for vibrations of thick laminated composite plates, Comput. Struct. 36(1), 57-64 (1990)

[14] Shiau L C. and Chang J T., Transverse shear effect on vibration of laminated plate using higher-order plate element, Comput. Struct. 25(2), 735-740 (1991)

[15] Tessler A., Saether E. and Tsui T., Vibration of thick laminated composite plates, J. of Sound & Vib. 179(3), 475-498 (1995)

[16] Attaf B., Effects of laminate stacking sequence on the free vibration of carbon/epoxy plates subjected to in-plane loads, La Recherche Aerospatiale, N°2, 149-153 (1996)

[17] Reddy J N. and Phan D N., Stability and natural vibration of isotropic, orthotropic and laminated plates according to a higher-order shear deformable theory, J. of Sound & Vib. 98, 157-170 (1985)

[18] Pervez T. *et al.*, Analysis of thick orthotropic laminated composite plates based on higher order shear deformation theory, Composite Structures, Vol. 71, n°3-4, 414-422 (2005)

[19] Yang P C., Norris C H.and Stavsky Y., Elastic wave propagation in heterogeneous plates, Int. J. Solids Struct., 2, 665-684 (1966)

[20] Yang T Y., *Finite element structural analysis*, Prentice-Hall, Inc., New Jersey (1986)

[21] Zienkiewicz O C. *et al.*, *The finite element method: its bases and fundamentals*, Elsevier Butterworth-Heinemann, ISBN 0 7506 6320 0, Oxford (2005)

[22] Burgoyne C J. and Crisfield MA., Numerical integration strategy for plates and shells, Int. Journal for Numerical Methods in Eng., Vol. 29, 105-121 (1990)

[23] Bathe K J. and Wilson E L., *Numerical methods in finite element analysis*, Prentice-Hall (1976)

How to cite this article
Attaf B and Bachene M. Effects of geometric ratios and fibre orientation on the natural frequencies of laminated composite plates. J Fundam Appl Sci. 2010, 2(2), 203-216.